Numerical modeling of the splitting of magnetic droplets by multiphase lattice Boltzmann equation

Clime, L.; Brassard, D.; Veres, T.

Publisher's version / la version de l'éditeur:
Journal of Applied Physics, 105, 7, pp. 07B517-07B520, 2009

Web page / page Web
http://dx.doi.org/10.1063/1.3068486
http://nparc.cisti-icist.nrc-cnrc.gc.ca/npsi/ctrl?action=rtdoc&an=10976303&lang=en
http://nparc.cisti-icist.nrc-cnrc.gc.ca/npsi/ctrl?action=rtdoc&an=10976303&lang=fr

Numerical modeling of the splitting of magnetic droplets by multiphase lattice Boltzmann equation

L. Clime,[a] D. Brassard, and T. Veres
NRC, Industrial Materials Institute, 75 Boul. de Mortagne, Boucherville, Quebec J4B 6Y4, Canada

(Presented 12 November 2008; received 17 September 2008; accepted 5 November 2008; published online xx xx xxxx)

A multiphase lattice Boltzmann numerical model driven by an isothermal interaction potential is applied for the splitting of magnetic droplets in electrowetting-on-dielectric devices. A hydrophilic magnetic plug is considered inside the liquid droplet and successive uniform force fields are applied in order to split this droplet. The numerical results are compared with experiments on water droplets containing plugs of superparamagnetic beads and good agreement is obtained. © *2009 American Institute of Physics*. [DOI: 10.1063/1.3068486]

I. INTRODUCTION

Biological molecules are commonly detected by using certain labels such as fluorescent dyes or enzymes.[1] One important role in the design of biosensors is played by particles that can be spatially manipulated and confined in certain regions of the biochip by using external fields. Electric,[2] magnetic,[3–5] or combinations of electric and magnetic fields[6] can be used in order to accurately manipulate and capture these particles. The magnetic labels are particularly advantageous since the magnetic background of biological fluids is very low and relatively large actuation forces can be obtained with relatively small (submicron-sized) magnetic particles.[7–9] Achieving high actuation forces is particularly important for bioassays performed in microfluidic devices. Indeed, in traditional continuous-flow microfluidic bioassays, the biological species are typically mixed and attached onto the surface of the particles, then flushed through microfluidic channels where coils and/or permanent magnets[3,7–9] are used to trap and confine the particles in certain regions where the detection has to take place. However, several issues related to the mixing (diffusion length) at very low Reynolds numbers[10] combined with the inherent difficulties in the design of scalable continuous-flow architectures[11,12] severely limit the reliability and throughput of magnetic-based bioassays performed in microfluidic channels. A better way to circumvent these drawbacks is to implement a chip architecture based on discrete droplets, namely, digital microfluidic based biochips. Unlike closed-channel flows employed in continuous microfluidics, digital microfluidic devices are based on discrete and independently controllable droplets that are manipulated on an open substrate by using external and completely reconfigurable controllers. Among the various mechanisms capable of manipulating and controlling liquid droplets on dielectric surfaces (dielectrophoresis,[13] thermocapillarity,[14] and surface acoustic wave transport[15]), the electrowetting effect (defined as the change in solid-liquid contact angle due to an applied potential difference between the solid and the liquid[16]) offers the distinct advantage of being highly suitable for large-scale integration on lab-on-chip device. Basic operations like transport, splitting, and merging of liquid droplets may easily be realized by simply applying appropriate voltages on the device electrodes.[17] Thus, magnetic beads can be confined to a single electrode with a concentrated magnetic field via a simple droplet merging and splitting routine.[17] Since the interfacial tension of the liquid plays a crucial role at this scale, the magnetically splitting of droplets charged with magnetic beads (henceforth referred to as magnetic liquids) will be the result between competing magnetic forces acting upon individual beads and overall interfacial forces at the contact lines with the dielectric platform. Obviously, proper designs of electrowetting devices needs deep understanding of both microscopic and macroscopic physics involved in these processes. Among the numerical techniques used to model the physical processes related to digital microfluidics, the lattice Boltzmann method (LBM) (Ref. 18) is a very promising tool, several theoretical[19] and experimental[20] confirmations being already reported in the literature. The main advantages of this method over other traditional techniques consist of its ability to easily address complicated processes related to liquid-vapor interfaces, multiphase and multicomponent flows, and contact line dynamics as well.

The aim of this work is to test the ability of a two-dimensional (2D) lattice Boltzmann scheme to satisfactorily reproduce the splitting of magnetic liquid droplets by electrowetting actuation and magnetic field gradients. Theoretical simulations are compared with experimental measurements in order to obtain the simulation parameters able to satisfactorily reproduce the observed experimental behavior.

II. EXPERIMENT

The experiment is performed on an EWOD (electrowetting-on-dielectric) microfluidic device consisting of an array of electrodes placed underneath a dielectric layer and covered by a thin hydrophobic coating [Fig. 1(a)].[21] The liquid droplets are "sandwiched" between the bottom substrate containing the electrodes and a top plate where a conductive thin film acts as a ground electrode. Water droplets of about 1.8 mm diameter and 150 μm height containing about

[a]Author to whom correspondence should be addressed. Electronic mail: liviu.clime@imi.cnrc-nrc.gc.ca.

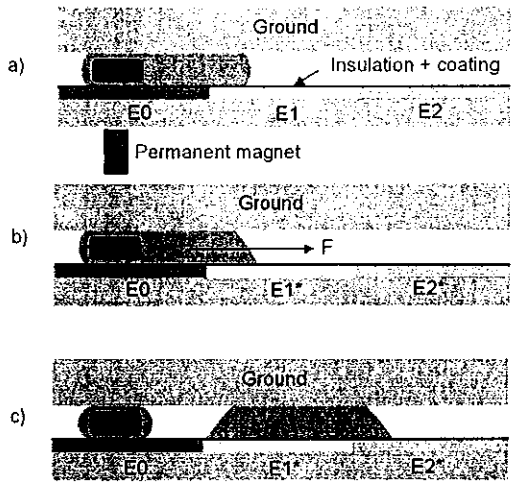

FIG. 1. (Color online) Schematic lateral view of a EWOD-based device for splitting magnetic droplets in magnetic and nonmagnetic counterparts. (a) A permanent magnet is placed underneath the bottom plate of the EOWD device in order to concentrate and retain the magnetic material of the liquid droplet above the electrode E0 only. (b) Electrodes E1 and E2 are activated by applying an electric potential with respect to the top (ground) plate. (c) The initial droplet is split in two smaller droplets: one containing the magnetic beads and another one completely nonmagnetic. Activated electrodes are indicated with star superscript symbols in their labels.

35 μg of 1 μm diameter superparamagnetic beads (Invitrogen[22]) are first introduced in the EWOD device. The actuation of the droplets (transport) is achieved by successively applying voltages on the bottom electrodes (E1, E2, etc.) with respect to the top electrode (ground). According to the electrowetting theory,[16] this potential modifies the contact angle of the liquid droplet with respect to the bottom plate coating layer, thus generating a net actuation force [Fig. 1(b)] toward these electrodes. The breakup of the initial droplet in two other smaller droplets, one containing the magnetic particles and another completely nonmagnetic [Fig. 1(c)], is realized when the external electrowetting actuation force is large enough to overcome the surface tension of the liquid. During this process, the magnetic force acting upon the plug of magnetic particles has to be large enough in order to hold back the droplet. A cylindrical permanent magnet with a diameter of 0.8 mm and a saturation magnetization of 1.4 T placed underneath the magnetic droplet [as schematically shown in Fig. 1(a)] is found to be powerful enough in order to concentrate and retain the magnetic plug during the splitting process.

III. NUMERICAL MODEL

The physical processes related to the electrowetting actuation and splitting of liquid droplets are modeled here with a D2Q9 LBM scheme[23] and a multiphase isothermal mesoscopic potential.[24] An array (computational domain) of 671×300 cells are filled with particles characterized by a Shan-Chen interaction potential[24] $\psi(\rho) = \psi_0 \exp(-\rho_0/\rho)$ where $\psi_0 = 4$ and $\rho_0 = 200$. Particles in these cells are distributed along nine well defined velocity directions (links) and their distributions updated according to the standard Bhatnagar–Gross–Krook collision rules.[23] Cohesion forces between fluid particles are then computed via

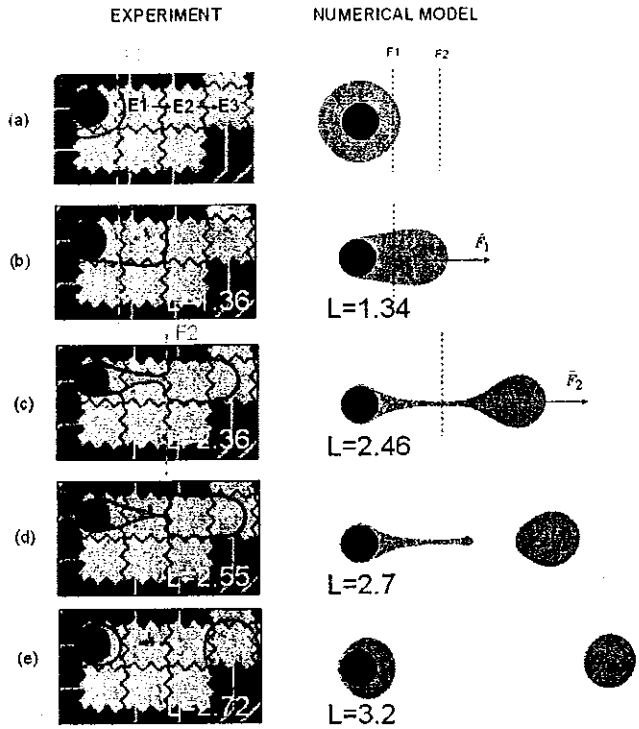

FIG. 2. (Color online) Splitting (top view) of a magnetic droplet on three electrodes: (a) magnetic beads (dark regions) in a single droplet above the permanent magnet, (b) electrode E1 is actuated and the liquid spreads on E1, while the magnetic plug remains confined in the region of high magnetic field gradient, (c) electrode E2 and E3 are actuated and the droplet form a dimmer of two smaller droplets linked by a very thin liquid filament, (d) the link between the two droplets is removed, and (e) two smaller droplets at different positions on the EWOD device are obtained. Experimental and theoretical total lengths (l) of the liquid droplet during the splitting process are indicated in (b), (c), (d), and (e).

$$F_{\text{fluid-fluid}}(\vec{r}) = -G_{LL}\psi_{\vec{r}}\sum_k w_k \psi_{\vec{r}+\vec{e}_k}\vec{e}_k, \quad (1)$$

where $G_{LL} = -120$ stands for the internal cohesion strength and is mainly responsible for the interfacial tension developed at the interface between two phases (here liquid and vapor). $\vec{e}_k$ and w_k are the unit vectors and the interaction weightings factor[19,24] corresponding to the link k of the cell located at $\vec{r}$, respectively. The adhesive interaction between fluid particles and the surface (the hydrophilicity) of the magnetic plug is modeled by analogy to fluid-fluid interactions,[25] by replacing G_{LL} in Eq. (1) with $G_{LS} = -350$ and setting $\psi = 1$ on all solid boundary nodes. In this way, the hydrophilicity of a certain material can easily be modeled by setting G_{LS} to a desired contact angle between the liquid and that material. In this work G_{LL} and G_{LS} are chosen in such a way that the contact angle of the liquid with respect to the magnetic plug be set to 0° (that is a very hydrophilic plug). This plug is represented in Fig. 2 as a dark disk of 50 lattice units (lu) diameter, surrounded by a liquid shell of total diameter $D_0 = 110$ lu. The interaction of the liquid droplet with the bottom and top plates of the devices cannot be directly introduced in 2D simulations. Thus, the electrowetting actuation force is modeled by vector fields acting on the liquid particles only ($\rho = \rho_{\text{liquid}}$) and located at regions corresponding to the actuation electrodes in the real device (the limits of these fields are denoted as F1 and F2 in Fig. 2). A force of

TABLE I. Physical quantities and numerical values of related LBM parameters responsible for the dynamics of the splitting of a magnetic droplet in a EWOD-based microfluidic device. In the expression for the magnetic force at equilibrium H_r stands for the radial magnetic field, ∇_r for its gradient in the plane of the EWOD device, V for the total volume of magnetic material in the droplet, whereas μ_0 and χ are the vacuum absolute magnetic permeability and apparent magnetic bead susceptibility, respectively.

Physical quantity	Experiment	LBM parameter
Diameter of magnetic plug	0.5 mm	50 lu
Diameter of droplet	1.5 mm	110 lu
Interfacial tension	0.073 N/m	14.3 lu mu ts^{-2}
Magnetic plug hydrophilicity	Contact angle: 0°	$G_{LS}=-350$
Magnetic force at equilibrium	$\mu_0\chi V(H_r\times\nabla_r)H_r\cong 2$ μN	$F_1=0.005$ mu lu/ts^2
Experiment time	200 ms	100 000 ts

0.005 mu lu/tu^2 is initially applied to the right side of the level F1 followed by another one of 0.01 mu lu/tu^2 at F2. This field sequence is considered to acceptably reproduce the experimental conditions in which lines of electrodes near magnetic droplet (like E1-E2-E3 in Fig. 2) are successively activated until a complete breakup of the droplet is obtained. Fully periodic boundary conditions[24] are imposed on all sides of the computational domain. After the simulation is initialized, a thermalization period of about 10 000 ts (1 ts = 1 LB iteration) is considered before the simulation starts and the force field sequence F1-F2 is applied. The numerical values of the parameters used in simulation are summarized in Table I in correspondence with the related physical quantities. On a shared memory supercomputer with quad-core Itanium microprocessors at 1.5 GHz each, the simulation time for the present droplet breakup is about ten central processing unit hours.

IV. RESULTS AND DISCUSSIONS

The breakup of a magnetic droplet in EWOD-based microfluidic devices is shown in Fig. 2. The left column of this figure contains top view images recorded with a high speed camera during the experimental splitting process, whereas the right column contains snapshots of the density field in the computational domain during the numerical simulation. In a first step, a positive voltage (90 V) is applied on the electrode E1 [Fig. 1(a)]. The liquid droplet spreads on this electrode but the magnetic beads are retained above the initial electrode due to the magnetic field created by the permanent magnet and an equilibrium state with an eccentric magnetic plug is obtained [Fig. 2(b)]. The corresponding numerical simulation in this figure is generated by applying a uniform scalar field of 0.005 mu lu/ts^2 at each lattice cell representing a liquid point. This stable configuration can be used in order to evaluate the minimum magnetic force required to hold back the magnetic plug. For the superparamagnetic plug and the permanent magnet used in this experiment, finite element simulations of the magnetic field generated by the permanent magnet suggest a retaining radial force of about 2 μN. Since the activation of one neighbor electrode is not enough in order to break up the magnetic droplet, the process is continued by activating the electrodes E2 and E3 and deactivating E1. In this process, the breakup of the droplet is fully realized [Fig. 2(e)] by some intermediary steps in which two smaller droplets are first linked by a very thin liquid filament [Fig. 2(c)] and then separated by the breakup of this link [Fig. 2(d)]. The accuracy of numerical simulated splitting process is evaluated by comparing total lengths (L) of the droplets and filament thickness (t) with experiments. These two quantities are both normalized to the diameter of the magnetic plug (D) and presented in Figs. 2 and 3 as numerical values and graphical representations, respectively. The agreement between numerical values of L in Fig. 2 is very good except Fig. 2(e) where a noticeable difference of about 18% with respect to the experiment is observed. This difference may be explained by the fact that in the EWOD device the droplet remains stuck above the last activated electrode (E3), whereas in the simulation, the liquid is allowed to freely move even after the breakup. The accuracy of the numerical model is further investigated by comparing the thicknesses of the droplet along its transversal direction at different splitting stages with the experiment (Fig. 3). A good agreement is obtained if the simulation time is normalized to 20 000 tu (iterations) and the real time to 25 ms. This means that in this process, a lattice Boltzmann iteration corresponds to 1.25 μs. It is worth mentioning that even the eccentricity of the magnetic plug in the final equilibrium state after the droplet breakup is well reproduced by the present model. However, some differences between the shapes of modeled and experimental droplets are observed and are being attributed to (i) the finite size of the electrodes in the real EWOD device and (ii) the use of a semi-infinite force vector fields rather than fully three-dimensional (3D) schemes for the electrowetting effect.

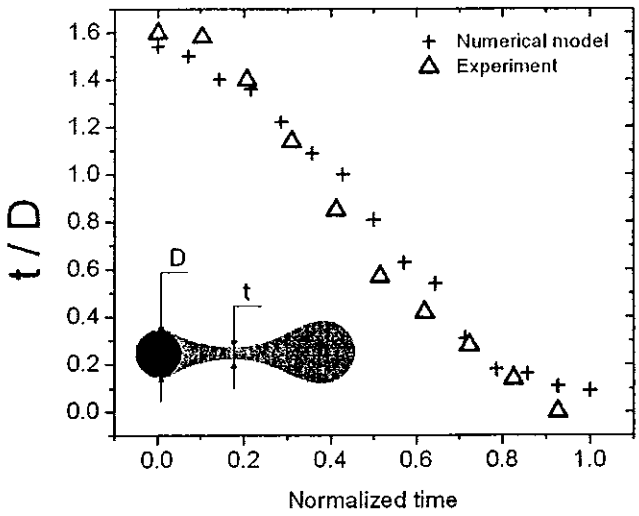

FIG. 3. (Color online) Experimental (open triangles) and numerical (full circles) values of the liquid filament thickness (t) to magnetic plug diameter (d) ratio at different stages of the breakup process starting with the application of the field F_2 (stage b in Fig. 2). Time on the abscissa is normalized to 20 000 tu (iterations) for the numerical simulation and 25 ms for the experimental values.

V. CONCLUSIONS

We presented a LBM-based numerical approach to the splitting of magnetic droplets in EWOD-based microfluidic devices. The simulation parameters able to accurately reproduce the dynamics of the breakup process are presented in relation with their corresponding physical quantities. Since the droplets in these microfluidic devices are extremely flattened (the form factor is about 1:10), 2D numerical schemes may give enough insight into the physical processes related to transport, splitting, or merging droplets. The challenge in using these 2D schemes instead of fully 3D models consists of accurately implementing the actuation scalar fields generated by the activation of the metallic electrodes.

ACKNOWLEDGMENTS

AQ: #1 The authors thank Réseau québécois sur les matériaux de pointe (RQMP) for providing access to their computational facilities. This work is supported by a joint grant from the Natural Sciences and Engineering Research Council and the National Research Council of Canada.

[1]D. Wild, *The Immunoassay Handbook*, 3rd ed. (Elsevier, New York, 2005).
[2]T. B. Jones, *Electromechanics of Particles* (Cambridge University Press, Cambridge, 1995).
[3]N. Pamme, Lab Chip **6**, 24 (2006).
[4]T. Vilkner, D. Janasek, and A. Manz, Anal. Chem. **76**, 3373 (2004).
[5]T.-Y. Ying, F. Prenger, L. Worl, M. Johnson, J. Waynert, and R. Wingo, Sep. Sci. Technol. **39**, 2915 (2004).
[6]L. Clime and T. Veres, J. Colloid Interface Sci. **326**, 511 (2008).
[7]L. Clime, B. Le Drogoff, and T. Veres, IEEE Trans. Magn. **43**, 2929 (2007).
[8]L. Clime, B. Le Drogoff, S.-Y. Zhao, Z. Zhang, and T. Veres, Int. J. Nanotechnol. **5**, 1268 (2008).
[9]B. Le Drogoff, L. Clime, and T. Veres, Microfluid. Nanofluid. **5**, 373 (2008).
[10]R. F. Ismagilov, J. M. K. Ng, P. J. A. Kenis, and G. M. Whitesides, Anal. Chem. **73**, 5207 (2001). AQ: #2
[11]M. G. Pollack, A. D. Shenderov, and R. B. Fair, Lab Chip **2**, 96 (2002).
[12]V. Srinivasan, V. K. Pamula, M. G. Pollack, and R. B. Fair, Proceedings of the microTAS, 2003 (unpublished).
[13]P. R. C. Gascoyne and J. V. Vykoukal, Proc. IEEE **92**, 22 (2004).
[14]A. A. Darhuber, J. P. Valentino, S. M. Trojan, and S. Wagner, J. Microelectromech. Syst. **12**, 873 (2003).
[15]A. Renaudin, P. Tabourier, V. Zhang, C. Druhon, and J. C. Camart, *Plateforme SAW Dédiée à la Microfluidique Discrète Pour Applications Biologiques* (Société Hydrotechnique de France, Paris, France, 2004), p. 14.
[16]G. Beni and S. Hackwood, Appl. Phys. Lett. **38**, 207 (1981).
[17]R. B. Fair, Microfluid. Nanofluid. **3**, 245 (2007).
[18]S. Chen and G. D. Doolen, Annu. Rev. Fluid Mech. **30**, 329 (1998).
[19]P. Raiskinmäki, A. Shakib-Manesh, A. Jäsberg, A. Koponen, J. Merikoski, and J. Timonen, J. Stat. Phys. **107**, 143 (2002).
[20]J. Hyvaluoma, A. Koponen, P. Raiskinmaki, and J. Timonen, Eur. Phys. J. E **23**, 289 (2007).
[21]D. Brassard, L. Malic, F. Normandin, M. Tabrizian, and T. Veres, Lab Chip **8**, 1342 (2008). AQ: #3
[22]Invitrogen www.invitrogen.com.
[23]Y. H. Qian, D. d'Humieres, and P. Lallemand, Europhys. Lett. **17**, 479 (1992).
[24]X. W. Shan and H. D. Chen, Phys. Rev. E **47**, 1815 (1993).
[25]N. S. Martys and H. Chen, Phys. Rev. E **53**, 743 (1996).